Lühr, B.-G., Koulakov, I., Rabbel, W., Zschau, J., Ratdomopurbo, A., Kirbani Sri Brotopuspito, Pak Fauzi, Sahara, D. P. (2013): Fluid ascent and magma storage beneath Gunung Merapi revealed by multiscale seismic imaging. - Journal of Volcanology and Geothermal Research, 261, 7-19

DOI: 10.1016/j.jvolgeores.2013.03.015

Fluid ascent and magma storage beneath Gunung Merapi revealed by multi-scale seismic imaging

Birger-G. LUEHR[1], Ivan Koulakov[2], W. Rabbel[3], Jochen Zschau[1], Antonius Ratdomopurbo[4], Kirbani Sri Brotopuspito[5], Pak Fauzi[6], David P. Sahara[7]

1 Helmholtz Centre Potsdam GFZ German Research Centre for Geosciences, 14473 Potsdam, Germany, email: ase@gfz-potsdam.de)

2 Inst. of Petroleum Geol. & Geophys., SB RAS, 3, Novosibirsk, 630090, Russia

3 Institute of Geosciences, CAU, Otto-Hahn-Platz 1, 24098 Kiel, Germany

4 EOS, Nanyang Techn. University, 50 Nanyang Avenue, Block N2-01a-15, Singapore 639798

5 FMIPA, Universitas Gadjah Mada, Sekip Unit III, Yogyakarta 55281, Indonesia

6 Meteorological & Geophys. Agency (BMG), Jl Angkasa I, Kemayoran, Jakarta 10720, Indonesia

7 Dept. Geophys. & Meteorology, Inst. of Technology Bandung (ITB), Bandung 40132, Indonesia

Abstract

Magma is fed to a volcano through a complex "plumbing" system that involves not only shallow structures beneath the volcano edifice, but also deep structures and processes within the underlying crust and upper mantle. This paper summarizes seismic experiments carried out over many years at Gunung Merapi in Central Java. These have resolved the 3D seismic velocity structure of the Merapi edifice, and provided a 3D structural image of the lithosphere and subduction zone beneath Central Java. Earthquake locations reveal that with distance from the trench, the dip of the subducting slab steepens from nearly horizontal (0-150 km), through 45 degrees (150 - 250 km), to 70 degrees (>250 km). The slab appears as a 30 km thick double layer of seismicity in a depth range of 80 km to 150 km, and it can be identified seismically to a depth of more than 600 km. The active volcanoes of Merapi, Sumbing, and Lawu are located at the edge of a large low velocity body that extends from the upper crust to the upper mantle beneath Central Java. Shear wave signals recorded above this anomaly are strongly attenuated compared to neighboring areas. The anomalous body

has a detected volume of >50,000 km^3 and a decrease in P and S velocities relative to adjacent regions of up to 30%. The resulting Vp/Vs ratio of up to 1.9 is unusually high for lower crust. Additionally, the anomaly extends along a 45 degree-slope downward from beneath the volcanic arc and meets the slab at 100 km depth. We interpret this sloping anomaly as a pathway for fluids and partial melts. Increased seismicity is observed at depths of ~100 km, possibly as a result of dehydration of the subducting slab with related fluid releases causing partial melting of overlying mantle material. The large velocity reduction and high Vp/Vs ratio in the region are consistent with an increase in temperature, a reduction of shear strength, and the presence of fluids or melts of 13 to 25 vol. %. The detected strong anomaly beneath Central Java is unique in size and amplitude compared to other subduction zones. The geophysical evidence suggests that this segment of the arc has a high magma flux and is thus capable of developing even larger shallow crustal reservoirs and more voluminous explosive eruptions in the future.

1. Introduction

Gunung Merapi, located in Central Java, is one of the most active volcanoes in the world. It is one of ~98 active volcanoes located along the Sunda Arc (*Simkin and Siebert, 1994*), a 5,000-km-long collision belt between the Eurasian and the Indo-Australian tectonic plates (Figure 1), where the Australian plate is being subducted beneath the Sunda block at a rate of about 6.5 cm/year (*DeMets et al., 1990*). Merapi's dominant type of volcanism is andesitic and its frequent eruptions threaten the surrounding densely populated area, mainly with pyroclastic flows, surges and lahars. For decades, researchers have investigated this volcano to understand the dynamics and structure of its magmatic system. Such knowledge about the volcanic system provides an important framework for improved assessment of related hazards.

The high seismic and volcanic hazard potential of Central Java was demonstrated by the disastrous Bantul earthquake (M=6.3) on May 26, 2006, which resulted in 5,750 fatalities, and most recently by the last eruption of Gunung Merapi in late October and early November 2010. This last eruption was unusually strong, classified as a VEI 4 event, comparable to the eruption of 1872. The volume of erupted lava of about 0.12 cubic kilometres (*Surono et al., 2012*) was ten times larger than all other eruptions during the 20th century. Pyroclastic density currents ran out to 16 km from the summit and devastated populated areas.

Fortunately, due to telemetric data from monitoring instruments analyzed by Indonesian experts and satellite radar data on the rate and size of a rapidly growing summit lava dome, an exclusion zone around the southern slope of the volcano was increased finally to a radius of 20 km prior to the paroxysmal eruption on 4-5 November 2010. As a result of the eruption, a total of about 400,000 residents were displaced according to data from Indonesia's National Agency for Disaster Management (BNPB; see also *Mei et al., 2013*), and only 367 people lost their lives. Approximately 10,000 to 20,000 lives were likely saved by the accurate eruption forecast (*Surono et al., 2012*).

Here we provide a broad geophysical context for future studies of Merapi, and the other papers in this special issue, by summarizing our current understanding of structure of the crust and mantle beneath Central Java. Our review is based heavily on our previous geophysical studies (Koulakov et al., 2007, 2009b, Wagner et al., 2007). The ascent of fluids and the formation and distribution of partial melts in the crust can be detected by seismic and seismological methods, and imaged with seismic tomography. In particular, as has been shown elsewhere in volcanic arcs, areas of partial melt are indicated by reduced seismic velocities and attenuation of seismic waves.We firstly focus on results from studies of global seismological data, local earthquake tomography of Central Java, and gravity modelling – studies that have revealed the geometry of the subducting slab beneath the magmatic arc. We then present a regional scale tomographic structure of the Java subduction zone section in which Merapi is embedded, and we review the seismic experiment (*MERAMEX* project) carried out to investigate the structure beneath Central Java. We then focus on the region directly beneath Merapi by presenting results from seismic studies that were particularly designed to illuminate the deep structure and magmatic plumbing of the volcano. Finally, in the discussion section, we combine the seismic results with petrological findings on magma genesis in order to arrive at new conclusions on the dimensions, depths and hazard potential of the Merapi volcanic zone.

2. The Central Java subduction zone

2.1. Distribution of slab-related seismicity

The largest databank of worldwide seismicity is the ISC catalogue (*ISC 2001*), which includes information on earthquakes and travel times of recorded seismic waves since 1964. The ISC catalogue data provide fairly good coverage in most seismically active regions of the world, which makes it suitable for performing tomographic inversions on regional and global scales. However, the data quality in the initial ISC catalogue is rather poor due to a significant amount of erroneous data, which may bias the locations of sources. Therefore, special efforts have been made to reprocess the ISC catalogue and as a result many specialists use a relocation method developed by Engdahl, van der Hilst, and Buland (the EHB method, *Engdahl et al., 1998*). With these or similar corrections, the revised ISC catalogue is widely used for earthquake analysis and tomographic inversion. In our studies, we used a similar relocation method developed by Koulakov and Sobolev (*2006*), which is specially oriented to detection and rejection of outliers in the data. The locations of events according to this procedure are based on travel times in a 1D spherical velocity model (here AK135 by *Kennett et al., 1995*) corrected for the Earth ellipticity, station elevations, and Moho depth.

In Figure 2 we present the distribution of seismicity beneath Java from the revised ISC catalogue for the period from 1964 to 2001, consisting mainly of large and moderate events recorded by worldwide networks. Despite our pre-processing, the location quality of these events is still low compared to the locations determined with data from the *MERAMEX* project, which used more than 100 local stations temporarily installed in Central Java (see description of *MERAMEX* in section 6). However, the very long period of recording makes the ISC data more representative. For example, due to the relatively short five month period of the *MERAMEX* project relative to the periodicity of seismicity along the arc, some seismic clusters in Figure 2 are poorly defined by *MERAMEX*, but well defined in the longer term ISC catalogue. Thus, both global and local catalogues provide valuable data which supplement each other.

It can be seen in Figure 2 that the events form clearly separated linear segments which mark the seismicity in different depth intervals. Shallow seismicity (down to 50 km depth) occurred mostly along the trench and in the accretionary prism beneath the offshore area. We suggest that the shallow seismicity in these areas is related to a high asperity of the slab, which generates strong stresses and resulting deformation in the overriding plate above the shallowest segments of the subducting slab. Note that the record presented in Figure 2 stops at 2001; it does not include the M 6.3 Bantul earthquake of 27 May 2006. The area where this onshore event took place, southeast of Merapi, had little seismicity during the years 1964-2006. This suggests that the crustal stresses released during this event had accumulated for fairly long time, i.e., more than the forty year coverage of the ISC catalogue.

Based on Figure 2 we can define several deep clusters of slab-related seismicity beneath Java. The first level corresponds to a 50-100 km depth interval (purple zone) that is observed beneath the offshore part south of Java. The second zone is located along the southern coast of Java at a depth interval between 100 and 200 km (orange zone). The next zone is beneath the northern coast (red zone) at depths of 200 to 250 km. Finally, the deepest cluster is located along a fairly narrow zone beneath the Java Sea (brown zone) at 550-650 km depth. These four levels possibly mark the different stages of rock transformations occurring in the slab. It can be seen that most of the volcanoes of Java are located above the second seismic zone (orange) at 100-200 km depth.

In the distribution of seismicity in the 50-100 km and 100-200 km zones we observe a seismic gap beneath central Java that coincides onshore with the location of Merapi volcano. In addition, the oceanic plate subducting beneath Central Java is segmented into two subplates of considerably different ages (e.g. Müller et al., 1997). These two oceanic plate segments may be subducting independently of each other opening a lateral slab window located beneath the Merapi volcanic complex. This window could form the pathway for deep-sourced magmas (e.g., Costa et al., 2013) and may be the cause of the high eruption frequency of Merapi. Slab windows have been suggested previously as a mechanism to explain unusual characteristics of volcanic systems, for example for the Kluchevskoy volcano group in Kamchatka (e.g., Levin et al., 2003, Koulakov et al., 2011a,b).

2.2. Insights from regional tomography

Additional information regarding the geometry of the subducting slab can be determined from seismic tomography. There are several published global and regional models that provide consistent images of the subducted lithosphere beneath the Sunda arc (Bijwaard et al., 1998, Widiyantoro et al., 1999, Gorbatov and Kennett, 2003, Pesicek et al., 2008). Here, we present a model of P and S velocity anomalies based on travel time data from the revised ISC catalogue and calculated with an algorithm for regional tomographic inversion (*Koulakov et al., 2002;* Koulakov and Sobolev *2006*) for the Sunda Arc down to 1000 km depth. The inversion is performed in a series of overlapping circular windows using data on body waves that travel, at least partly, through the studied volume. We include rays from events located in the investigated region that are recorded by worldwide stations, and rays from remote events recorded by regional stations. This algorithm has been successfully implemented for studying the upper mantle beneath Europe (*Koulakov et al., 2009c*), Asia (*Koulakov, 2011*), Kurile-Kamchatka subduction zone (*Koulakov et* *al., 2011b*), and many other regions.

Our tomographic inversion results are presented in Figure 3. As in most previous tomographic studies, our P and S-seismic models for the Sunda Arc provide clear images of the subducting Indo-Australian plate, which is visible as a high-velocity anomaly aligned with seismicity in the Benioff-Wadati zone. However, some details in our model differ from the previously created models and provide new information on the structure of the slab. Here, we mostly focus on results related to the Central Java segment. In Figure 3 we present two vertical sections for P and S anomalies to the west and to the east of the Merapi. We can see that the slab appears to vary in thickness.

For the western section in the region from the surface down to 350 km depth, the slab is clearly imaged as prominent P and S anomalies. In the eastern section the anomalies are less prominent, especially the S-wave velocity anomaly. This diminution of the anomalies favours the hypothesis for a slab window beneath the Merapi area, as discussed in the previous section. This zone has a thickness of 200 km – thicker than expected for subducting oceanic lithosphere. The great thickness could result in part from a smearing effect due to insufficient model resolution; however, our synthetic tests show that smearing in this area is not a major factor. Another possible explanation is that unusual cooling of the mantle above and below the slab produces a much thicker high-velocity area than that of the slab itself.

Between 350 and 450 km depth, the slab-related high-velocity anomaly is weaker. We suggest that the lower velocity might be related to the geometry of olivine phase transition interfaces to spinel minerals, which theoretically begin at about 410 km depth. Seismic tomography is not capable of resolving the geometry of such first-order interfaces, but these features can bias a 3D velocity structure.

Below 450 km depth in both sections, we observe a large high-velocity anomaly, which extends to the base of the model at 1000 km depth. For the eastern section the high-velocity anomaly appears to be much thicker and appear as an isometric body rather than a slab. We propose that this large high-velocity body represents an accumulation zone for remains of the subducted slab. The transition of mantle minerals from spinel to perovskite at about 670 km depth should create a considerable density and viscosity contrast, such that the subducting plate cannot pass directly through this interface. In theory, only after a long period of crystallization of the denser perovskite phase a critical mass is generated such that the remains of the slab and surrounding upper mantle rocks can penetrate to the lower mantle (e.g., Goes et al., 2008). However, the process of dense-phase accumulation and descent is not synchronous beneath different segments of the subduction zone. Thus we observe rather big differences in the shape of the high-velocity body in the transition zone and uppermost part of the lower mantle. Similar features were observed in other subduction zones, such as beneath the Kurile-Kamchatka arc (*Koulakov et al., 2011b*).

Regional-scale seismic tomography, as well as the distribution of Benioff-Wadati seismicity from the revised ISC catalogue, provides the shape of the subducting slab down to 1000 km depth. However, the robustness of these determinations is much lower for the uppermost part of the model (roughly down to 150 km). This lack of robust data at this shallow depth interval is compensated by using the local earthquake data, which provide the fine structure of the slab-related Benioff-Wadati zone beneath Central Java and the Merapi.

As we can see from the results of regional tomography, the subducting slab cannot be represented by an oversimplified conveyer-type 2D model. The considerable lateral and vertical variations in the slab thickness probably have effects upon the surface tectonics. In particular, the arc volcanism, which is ultimately fed from the subducting slab, has a link with the slab behaviour. In particular, we believe that the specific character of Merapi volcano could be caused by a slab window formed in the contact zone between two autonomously subducting oceanic plates.

However, in the upper part of the mantle and even in the crust, the resolution of the global data cannot provide the detail we need to resolve the magmatic plumbing of the volcanic zone. This limitation led to a seismic tomography experiment, designed to resolve the crust and upper mantle below the volcanoes of Central Java from the surface down to 150 km depths (*Bohm et al., 2005*).

3. Imaging the crustal and upper mantle plumbing system beneath Central Java

3.1. The MERAMEX project

Between May and October 2004, combined amphibious seismological investigations at 110°E were performed as part of the *MERAMEX* (MERapi AMphibious EXperiment) project (*Reichert and Luehr, 2005*). The measurements were carried out in co-operation with Indonesian research institutions to investigate the tectonic setting and the volcanic feeding system beneath Central Java. A temporarily installed seismic network of 134 continuously recording stations (triangles in Figure 4), 106 short period Mark L4 seismometers, 14 broadband Guralp seismometers, 8 ocean bottom hydrophones (OBH), and 6 ocean bottom seismometers (OBS), covered a region of about 150x200 km. OBH's and OBS's were deployed during the RV SONNE cruise SO176 to extend the land network offshore to the south of Central Java. The average onshore station spacing was about 20 km. Two of the stations were installed 60 km to the north of the main network on the Karimun Jawa island group in the Java Sea above a cluster of hypocenters at 600 km depth. Offshore, the spacing of the ocean bottom instruments was about 40-90 km. Active seismic experiments were carried out offshore during a second cruise in September/October 2004, SO179. The amphibious data consist of 50,060 first arrival travel time picks of airgun shots fired along three seismic wide-angle profiles and recorded with the onshore *MERAMEX* network. Four to 5 local earthquake events could be recorded per day, in addition to regional and teleseismic events. The clearest signals were observed at southern and northern coastal areas. In the interior of Central Java, north to Merapi and Lawu volcanoes, the recorded shear wave phases were strongly attenuated. Thus, even a preliminary qualitative evaluation of the seismograms from the experiment showed that there is a significant anomaly beneath Central Java.

3.2. Results of the MERAMEX tomographic inversion

For the passive source tomographic inversion, 292 earthquake events were used. In total, 13,800 phases (8,000 P- and 5,800 S-phases) were selected for simultaneous iterative source location and tomographic inversion. A detailed description of this study can be found in Koulakov et al. (*2007, 2009b*). The P velocity reference model down to the depth of 20 km was estimated based on results of an active seismic experiment performed in the off-shore part of *MERAMEX* (*Wagner et al., 2007*). For deeper parts, no reliable constraints were available, therefore, for the range below 20 km depth, the velocity model was defined based on the global AK135 model (*Kennett et al., 1995*). A first S velocity distribution was determined according to a fixed Vp/Vs ratio of 1.74.

Final earthquake locations are shown in Figure 4 in map view (upper plot) and cross section (lower plot). In the vertical section of Figure 4 it can be recognized that the earthquakes line up along the Benioff-Wadati zone. The events depict variable dipping angles of the slab. For the first 150 km distance from the trench (50-250 km in the profile P1-P2) the slab appears to be almost horizontal. From 250 km to 450 km along profile P1-P2, the dip angle of the slab becomes about 45˚. Between 40 and 130 km depth this branch shows a rather clear double seismic zone with a thickness of 20-30 km that decreases with depth. Similar doubled seismicity zones with spacing of ~30 km have been observed at other subduction zones, e.g. Japan (*Okada and Hasegawa, 2000; Nakajima et al., 2001*), New Zealand (*Okaya et al., 2002*). It is assumed that the intermediate depth events are related to phase transition of blueshist to eclogite and to the deserpentinization of hydrated oceanic mantle (*Peacock, 1993, 2001, Gill, 1981*) and that the double seismic zone indicates isotherms in the subducted oceanic plate. In the depth interval from 250 to 600 km, the slab dips ~70˚.

Models of the anisotropic structure beneath central Java based on the local earthquake tomography (*Koulakov et al., 2009b*) are shown in Figures 5 and 6 for relative P (Vp) and S (Vs) velocity anomalies in horizontal and vertical sections. The reconstruction of relative anomalies even in highly heterogeneous areas was fairly stable and does not depend very much on the chosen reference model (*Koulakov et al., 2007*). A good spatial resolution was achieved down to 150 km.

The first striking feature is an almost perfect correlation of P and S anomalies in the crust. In the upper mantle, the correlation between P and S models is less clear. It might be caused by lower reliability of features in the uppermost mantle compared to crustal structures. The most prominent feature in the crust is a strong low-velocity anomaly (MLA, Merapi-Lawu Anomaly) with a reduction in velocity up to 30% for the P-model, and up to 36% in case of the S-model. The MLA fills the areas between the main volcanic complexes in Central Java. The largest part of this anomaly is located close to Merapi and Merbabu volcanoes (for short, Merapi complex), and extends to Lawu volcano in the east. The second, smaller part is between Merapi complex and the Sumbing-Sundoro-Dieng volcanic chain (for short, Sumbing complex). Between October 2011 and January 2012 the Indonesian Centre for Volcanology and Geologic Hazard Mitigation (CVGHM) reported increased activity for Sundoro. Surprisingly, the active volcanoes are not located above the central part of the anomaly, but surrounding it.

In the vertical sections (Figure 6), it can be seen that the MLA is inclined southwards towards the slab and extends into the upper mantle. The reliability of the models was tested comprehensively and carefully as described by Koulakov et al. (*2007, 2009b*). The most active volcanoes (Sundoro, Merapi, and Lawu) are located just above the contact region between this anomaly and the high-velocity forearc.

In the forearc, between the southern coast of Java and the volcanic arc, the crust appears to be highly heterogeneous. This may be due to alternation of highly deformed low-velocity limestone massifs and Cenozoic gabbroic intrusions (Rahardjo et al., 1995; van Bemmelen, 1949). However, in most parts, the link between geology and tomographic images is not clear, because the main geological structures of Central Java are covered by younger volcanic deposits and sediments.

Anomalies within the slab could not be resolved, because events in the Benioff-Wadati zone are located mainly at the uppermost boundary of the slab. Therefore, only few upward travelling seismic rays pass through the slab, and the corresponding travel time data provide almost no information about the inner structure of the slab.

3.3. Gravity modelling

The obtained seismic anomalies were compared with the Bouguer gravity anomalies of Smith and Sandwell (1997), as illustrated in Figure 7A. It can be seen that the main features of gravity and seismic models correspond well to one another. For example, the strong negative seismic anomaly located north of Merapi and Lawu volcanoes (MLA) corresponds to a negative gravity anomaly. In the forearc, dominantly positive seismic anomalies correspond to positive gravity anomalies. To quantify this link, we have performed gravity modelling with the aim of estimating values of $d\rho / dv$ coefficients (anomalies of density over anomalies of seismic velocity) for different crustal zones. When performing this modelling, we presume that on this scale of anomalies, the observed gravity effect is only due to the crustal patterns; the mantle anomalies were not included in the modelling.

For the modelling, the crust was subdivided into several zones representing the main geological and geophysical features. For example, zones 1 and 2 represent two segments of the offshore crust, zone 3 corresponds to the onshore part of the forearc, zone 4 passes through the main arc volcanoes in Central Java, zone 5 coincides with the MLA and low-gravity anomaly, zone 6 represents the onshore backarc area, and zone 7 is located in the offshore area north of Java. The contours of these zones are shown in Figure 7B and C. All zones were defined down to 25 km depth. The gravity effects of each of these zones were computed separately by using P or S anomalies obtained from local earthquake tomography (Figure 5) and by assuming constant values for the coefficients converting seismic velocity to density. Calculations of the gravity effect on the surface from 3D velocity distributions were performed by using a direct 3D integration in a regular grid. Then the gravity effects of all zones were summed with manually defined $d\rho / dv$ coefficients for each zone. The values of these parameters were optimized to achieve the best fit of the observed and computed gravity fields. The final computed gravity fields derived from the P- or S-velocity anomalies are shown in Figure 7 B and C.

Although the derived coefficients determined by this modelling are not expected to be highly accurate, they do provide semi-quantitative information concerning geological processes in the crust of Central Java. The highest values for the P and S models are obtained for zone 3, representing the forearc. Here, the seismic anomalies are mostly caused by alternation of sedimentary and igneous rocks, which give much stronger differences in density than in seismic velocities. For the arc anomalies and for the MLA (zones 4 and 5) the values of $d\rho / dv$ are quite low. Volcanic conduits in these zones contain magma and other fluids, materials that can produce a strong decrease of seismic velocities. In addition, the integral effect of a sharply heterogeneous crust in these zones also contributes to a general decrease of seismic velocity. However, these structures are not always related to significant low densities. In zone 6 the correlation of gravity and seismic anomalies is low which explains a low value of the $d\rho / dv$ coefficient.

4. The Internal Structure of the Merapi edfice

4.1. The MERAPI project

During the past several decades many research projects have yielded information about the eruption history, volcanic processes, magmatic evolution, and internal structure of Merapi. These studies have had a common goal of contributing to an improved hazard assessment. The *MERAPI* (Mechanism Evaluation, Risk Assessment, and Prediction Improvement) project (1997-2002) was one of these activities, providing a better understanding of the eruption history and the explosive behaviour, thereby contributing to an improved early warning capability, and risk assessment (*Zschau, et al., 1998, 2003; Gertisser and Keller, 2003*).

Merapi is known as a frequently erupting volcano, with 105 to 108 eruption phases during the Holocene (Siebert et al., 2010; c.f., Badan Geologi, 2011). Small eruptions have occurred every two to five years, while larger eruptions occurred in 50 to 80 year intervals. Historically, 71 eruptions were documented since the year 1548 with the most violent ones in 1786, 1822, 1872, 1930, and 2010. The volume of erupted material compared to other volcanoes is low. The annual erupted volume is in a range of 1.2 million cubic meters of potassium rich basaltic andesite with varying SiO_2 content (52 – 57 wt. %) (Siswowidjoyo et al., 1995; Andreastuti et al,, 2000; *Gertisser and Keller, 2003*).

4.2. Geophysical results for Merapi edifice

For a better understanding of the volcanic activity, the geophysical structure of the volcanic edifice was intensively investigated (*Müller and Haak, 2004; Müller et al., 2002; Wegler and Lühr, 2001; Maercklin et al., 2000*) with a particular focus on imaging the magmatic system. Seismological investigations carried out by Ratdomopurbo and Poupinet (*1995*) revealed a zone with unexpectedly low seismic activity at a depth of 1-2 km, just below the summit. Ratdomopurbo and Poupinet (*1995*) associated this zone with a shallow magma reservoir (Figure 8), while a deeper chamber was assumed to lie at depths extending to 10 km or more. Later, the hypothesis of a deeper chamber was supported by petrologic data (*Purbawinata et al., 1997*), and several additional petrologic studies have shown that Merapi magmas are staged at multiple levels, ranging from the shallow conduit down to ~30 km (*Chadwick et al., 2007, 2008; Deegan et al., 2011; Costa et al., 2013*). On the basis of modelling GPS and tilt data, Beauducel and Cornet (*1999*) concluded that the magma reservoir responsible for feeding the eruptions of the 1990's was located between 6 km to 9 km below summit. In addition, high resolution gravity modelling (*Tiede et al., 2005*) provided evidence for high-density bodies, which may be interpreted as solidified magma intrusions or former reservoirs beneath the summits of Merapi, Merbabu, and Telemoyo volcanoes.

In contrast to the work by Ratdomopurbo and Poupinet (1995), geoelectric soundings and active seismic investigations (*Wegler et al., 1999; Wegler and Lühr, 2001*) have found no evidence for a shallow magma reservoir within the edifice. Instead a 4 km wide structure in the centre of the edifice with reduced seismic velocity and high electrical conductivity (*Müller and Haak, 2004*) was interpreted as a narrow alteration zone surrounding the conduit where conductive fluids circulate (*Maercklin et al., 2000, Müller et al., 2002*). Precise investigations of soil temperature and CO_2 gas flux at the summit area carried out during the inter-eruption period of 2002 to 2007 (*Toutain et al., 2009*) support this idea. This study found degassing anomalies that appear to be controlled by structures identified as concentric historical caldera rims (1932, 1872, and 1768), which have undergone a hydrothermal self-sealing process that lowers permeability and porosity. Variations of fluid mass contents in these regions are sufficient to explain observed gravity changes (*Westerhaus et al., 2007*). Based on these findings and those by Ratdomopurbo and Poupinet (*1995*), it was suggested that volcanic earthquakes could not be generated at depths much greater than 5 km, because the aseismic main "magma chamber" is located below this depth.

Gossler (*2000*) analyzed teleseismic events recorded at the broadband stations of the *MERAPI* monitoring network with the Receiver Function method. However, the results revealed little about the shallow structure – a result that we now know is due to a highly complicated structure beneath Merapi. In addition, limitations of the method itself precluded any detailed insights about the deeper structure. Besides, the heterogeneous eruptive material of Merapi, like alternating deposits of pyroclastic flows, lahars, ash falls, and lava flows, causes strong multi scattering effects on seismic waves (*Wegler and Lühr, 2001; Wegler et al., 2006*). The seismograms from artificial aigun shots (*Wegler, et al., 1999*) recorded on the slopes of Merapi volcano are characterized by spindle-like envelopes, small or missing P- wave onsets, missing S-wave onsets, and long codas, and demonstrate, that multiple scattering is an important effect, which cannot be neglected in the modelling of seismic wave propagation at Merapi volcano. Assuming the dominance of shear waves in the coda and a typical S-wave velocity of around 1.5 km/s for the shallow volcano this corresponds to a transport mean free path length L of only 0.1 km, which is 3 orders of magnitude smaller than for normal Earth crust, where L is typically of the order of 100 km. The corresponding length scales for intrinsic attenuation derived for Merapi volcano depend on frequency and are at least one order of magnitude larger than the transport mean free path (*Wegler and Lühr, 2001*). Magnetotelluric and geomagnetic profiles were carried out crossing Central Java (*Hoffmann-Rothe et al., 2001*). Modelling of the data revealed zones of high electrical conductivity in the upper crust, but the depth penetration faded away below a few kilometres. Consequently, there was little geophysical information about the deeper parts beneath Merapi and Central Java until the more recent, larger-scale seismic experiments described in Sections 2 and 3 above.

5. Discussion

Syracuse and Abers (*2006*) have analyzed the variations in vertical distance between arc volcanoes at the surface and the slap at depth for nearly all subduction zones. They found that the average slab depth is around 100 km below the volcanoes. Discrepancies were found only in a few cases, as in Central Java, where the vertical distance from the surface to the slab is around 150 km. They attempt to explain such deviations from the average depth by calling on special physical conditions. Another common feature of subduction zones is the observation that earthquake hypocentre distributions show two maxima in depth. A shallow clustering around 20 to 50 km is related to tectonic stress release. Another increase in the frequency of earthquakes occurs at 100 km depth on average (*ISC, 2001*). This peak in seismicity is observed in the same depth range below Central Java.

In the Central Andes, seismicity clusters are found at 100-120 km beneath the main volcanic arc linked with low P- and S-velocity zones (*Dzierma et al., 2012; Koulakov et al., 2006; Schurr et al., 2003; Husen and Kissling, 2001*). It is presumed that these zones trace the upward migration of fluids released from the slab due to phase transitions. These ascending fluids cause decreasing viscosity, and possibly, partial melting. The partially molten materials penetrate into the crust and form magma reservoirs, and in some cases ascend to the surface and cause volcanic eruptions.

The most important feature of the *MERAMEX* tomographic models is an unusually strong low-velocity anomaly located in the backarc crust just north of the volcanoes Sumbing, Merapi, and Lawu (Figures 5 and 6). The main part of this anomaly extends about 80 km from east to west and 30 km from north to south, as well as to a depth of over 50 km, from where it further extends as an inclined tongue with decreasing amplitude toward the slab at a depth of 100 km. The active volcanoes are located at the edge of this anomaly between high and low velocity regions. The low velocity body has a volume of more than 50,000 km^3 and is characterised by a reduction in velocity of up to 20% for the P-model, and up to 25% for the S-model. Shear wave signals recorded above this zone are strongly attenuated compared to areas outside the anomaly. Additionally, there is a good correlation between the distribution of velocity anomalies in the crust and gravity anomalies (*Untung and Sato, 1978; Smith and Sandwell, 1997*), as shown in the previous section. High-velocity seismic anomalies in the forearc correspond to gravity highs, and the low-velocity MLA fits well with a distinct gravity low (Figure 7). The low gravity region corresponds to the Kendeng Basin, which is located behind and aligned parallel to the volcanic front of Central and East Java. The Kendeng Basin succession is not well exposed but contains much volcanic debris. The deposits have an estimated thickness up to 10 km based on gravity modelling (*Waltham et al. 2008*). Consequently, we interpret this behind-the-volcanic-front anomaly as the combined product of a thick package of low-velocity sediments in the upper crust, as well as increased temperatures and magmatic fluids in the middle and lower crust.

As mentioned above, there is an increase in seismicity at a depth of around 100 km along the top of the down-going slab. This increase in seismicity can be explained by mineralogical phase transitions resulting in dehydration. Mineralogical investigations of Mierdel et al. (*2007*) provide a better understanding of the role of water and the storage capacity of water in minerals within the Earth’s shallow mantle. They showed that the ratio of water saturation versus depth has a pronounced minimum between 100 and 200 km (*Bolfan-Casanova, 2007*). Depending on the tectonic environment and temperature, the minimum in solubility may be shallow, as in the case of oceanic mantle, but deeper in case of cold continental lithosphere. We propose that for Central Java in a depth range near 100 km, where seismicity is increased, fluids (mainly water) are released from the slab and begin to ascend, leading to a reduction in melting temperature in the overlying mantle wedge (*Poli and Schmidt, 1995*). The ascent path is imaged tomographically as a zone of low seismic velocity. In the case of Central Java, this path is not vertical but has a 45 degree dip back toward the trench (Figure 9).

Synthetic tests (*Koulakov et al., 2007*) have proven that the MLA cannot be explained simply by a 10-km-thick low-velocity sedimentary basin (thickness inferred by gravity modelling; *Untung, M., and Y. Sato, 1978*). Such a basin, even with seismic velocities lowered by fluid or gas reservoirs, would not be able to generate the high amplitudes observed in our model down to depth of 20-25 km. Hence, the deeper parts of the crust must also have low velocities, and active seismic studies confirm this (*Wagner et al., 2007*). Unfortunately, aside from gravity modelling, which is non-unique with respect to source material, there is no other quantitative information about the thickness of the sedimentary basin in the literature. As mentioned above, the very low P- and S-velocities within the shallowest part of the MLA could in part result from a high content of fluids (gas and liquids) in the sediment layers. Mud volcanoes in northern Central Java with active release of methane favour this hypothesis.

The velocity perturbations, the attenuation of P- and S- waves, as well as the high Vp/Vs ratio of the MLA indicate a high Poisson's ratio of 0.3, and correlation with a gravity low indicates an area of increased temperature and reduced shear strength in the crust. Depending on the elastic modulus, a content of fluids and partial melts of 13% to 25% is estimated for the MLA volume. Possibly, the regions of the MLA below the sedimentary basin consist of a rigid matrix with pockets of magmatic mush or nearly molten material. The sediments my act as a seal so fluids from the mantle wedge just beneath the MLA cannot pass vertically to the surface. This hypothesis is indirectly supported by relatively strong, randomly looking travel time residuals after inversion (*Koulakov et al., 2007*). An explanation for this noise could be the existence of relatively small bodies of contrasting material causing scattering. They affect the travel times of seismic rays, but cannot be resolved by the tomographic inversion. On the hand, taking into account realistic frequencies of seismic signals from natural sources, a significant scattering induced effect on the travel time can be expected only for anomalies of a minimum diameter of 1-2 km. On the other hand, anomalies of 15-20 km would be resolved in the images and the signals would be more coherent. Therefore, we interpret the lower part of the MLA as a zone composed of a solid matrix, or "reservoir", that contains pockets of 2 – 15 km diameter that are filled with molten or partially molten material.

This model is supported by petrological investigations. Chadwick and Troll (*Chadwick et al., 2007*) found a lot of minerals in Merapi lavas crystallized at pressures of between 400 and 800 MPa, corresponding to a depth of 15–25 km, with a total range from 100 to 1,350 MPa, corresponding to a depth of 4-40 km. Similar wide ranges in petrologic equilibration depths were estimated by Costa et al. (*2013*). Two types of amphiboles are identified in the 2010 Merapi deposits, indicating depths ranges of crystallisation of 200 to 300 MPa (5 to 6 km depth) and 500 to 700 MPa (~10 to 20 km depth), respectively (*Surono et al., 2012; Costa, et al., 2013*). Furthermore, the analysis of Chadwick et al. (*2007, 2008*) and Deegan et al. (*2011*) indicate that Merapi eruptives are contaminated by crustal fragments in a depth range between 3 km and 11 km. The assimilated sediment fragments for instance contribute to CO_2 emissions at Merapi volcano. Significant contribution to the volatile budget of magma via limestone assimilation could have profound effect on our understanding of the driving mechanism of eruptions at Merapi and other volcanoes sited on carbonate crust. For example, the highly explosive 2010 eruption was preceded by increased CO_2 emissions, which were interpreted as the result of some combination of deep degassing of basaltic magma and limestone reaction (*Surono et al., 2012; Costa et al., 2013*).

Our synthesis model images a velocity section crossing Merapi (Figure 9), and demonstrates the link between volcanism in Central Java and the subduction process. Above 60 km depth, we observe an inclined negative velocity anomaly, most probably caused by fluids and partial melts ascending to the surface. When the fluids and melts reach the bottom of the rigid forearc, expressed by a positive velocity anomaly, they are not able to pass through. Instead they follow its bottom contour. Fluids probably behave in the same manner inside the MLA. As a result of such a migration from beneath the forearc and MLA, the highest concentration of melts would occur along the boundary between them. This appears to be the most favourable location for active volcanism where it is indeed observed today.

The velocity anomaly amplitudes found beneath Central Java are exceptionally high compared to anomalies found at other subduction zones. Toba volcano located in northern Sumatra is the source of the largest eruption on Earth within the last two million years. The resulting caldera is 30 x 100 km and has a total relief of 1,700 m. In one eruptive phase at around 75,000 BP, Toba produced the Young Toba Tuff, which has a volume of 2,800 km^3. Tomographic investigations of the Toba area (*Koulakov et al., 2009a*) lead to a model that images patches of negative anomalies beneath Toba with velocity reduction values not more than 15% (*Koulakov et al., 2009a*). Such a velocity reduction appears to be typical for volcanic areas at subduction zones, and for instance comparable to anomalies found in the Andes (Schurr et al., 2003; *Koulakov et al., 2006*) or Kamchatka (*Koulakov et al., 2011a*).

Therefore, if our model for magma and magmatic fluids being largely responsible for the MLA anomaly is correct, it raises an intriguing question: Can the fluids and melts within the MLA be mobilized in an eruption? We note that if only a few percent of fluids and melts in our model for the MLA were mobilized and erupted in a single event, it would be larger than the 100 km^3 Tambora eruption of 1815. Solving this question needs further interdisciplinary and multi-parameter investigations with a focus on this low-velocity anomaly now identified beneath Central Java.

6. Summary and Conclusions

(1) Seismic experiments carried out over many years at Merapi have resolved the 3D velocity structure of the volcano edifice, and provided a 3D image of the lithospheric structure and the subduction zone of beneath Central Java.

(2) Local earthquakes trace the subducting slab beneath Central Java as a 30 km thick double layer in a depth range of 80 km to 150 km. At a distance of up to 150 km from the trench, the slab is nearly horizontal. Between 150 km and 250 km distance, slab dip increases to 45 degrees and beyond 250 km it steepens to 70 degrees. The slap can be identified seismically to a depth of 600 km.

(3) A large low velocity body extends from the upper crust to the upper mantle beneath Central Java. The active volcanoes Merapi, Sumbing, and Lawu are located at the edge of this anomaly. Shear wave signals recorded above this anomaly are strongly attenuated compared to neighboring areas The anomalous body has a volume of >50,000 km^3 and a decrease in P and S velocities relative to adjacent regions of up to 30%. The resulting Vp/Vs ratio of up to 1.9 is unusually high for lower crust.

(4) A 45 degree-sloping anomaly extends downward from beneath the volcanic arc and meets the slab at 100 km depth. We interpret this sloping anomaly as an ascent pathway for slab-derived fluids and partial melts. Increased seismicity is observed at depths of ~100 km, possibly as a result of dehydration of

the subducting slab. Such dehydration releases fluids that ascend from the down-going slab, cause a decrease of melting temperature of overlying mantle material, and induce melting.

(5) The large velocity reduction combined with a high Vp/Vs ratio in the region below Central Java is consistent with an increase in temperature, a reduction of shear strength, and the presence of fluids or melts of 13 to 25 vol. %. The strong anomaly beneath Central Java is unique in size and amplitude compared to findings at other subduction zones. This suggests that this segment of the arc has a high magma flux and is thus capable in the future of developing even larger shallow crustal reservoirs and more voluminous explosive eruptions.

(6) A main conclusion of our work on Merapi and its surrounding is that the plumbing system of such highly active volcanoes cannot be seen solely from volcano-scale observation but must be understood within the regional tectonic context.

Acknowledgements

This research project was funded by the German Federal Ministry of Education and Research (BMBF) within the special program GEOTECHNOLOGIEN, and the GeoForschungsZentrum Potsdam (GFZ). Ivan Koulakov was supported by projects IP SB RAS #20 and ONZ-7.3 RAS. Essential support of the project was provided by the Center for Volcanology and Geologic Hazard Mitigation (CVGHM) Bandung, the Volcanological Technology Research Center (BPPTK) Yogyakarta, the Gadjah Mada University (UGM) Yogyakarta, Institut Teknologi Bandung (ITB) Bandung, and the Meteorological and Geophysical Agency (BMG) Jakarta. We would like to thank all Indonesian and German colleagues and students participating in the fieldwork. Instruments were provided by the Geophysical Instrument Pool Potsdam (GIPP), the Christian Albrecht University, Kiel, and the GEOMAR Helmholtz Center for Ocean Research, Kiel. Many thanks also to the reviewers for their critical, constructive and helpful comments. Our special thanks are going to John Pallister for his constructive support and hints, and to Eohan Hologhan for improving the structure of the manuscript and the English writing.

References

Andreastuti, S.D., Alloway, B.V., Smith, I.E.M., 2000. A detailed tephrostratigraphic framework at Merapi Volcano, Central Java, Indonesia: implications for eruption predictions and hazard assessment. Journal of Volcanology and Geothermal Research 100, 51–67.

Badan Geologi, 2011. Data Dasar Gunung Api Indonesia, Kementerian Energi dan Sumber Daya Mineral, Bandung, Indonesia, vol., 2, 522 pp.

Beauducel, F. and F.H. Cornet, 1999. Collection and three-dimensional modeling of GPS and tilt data at Merapi volcano, Java, J. Geophys. Res., 104, B1, 725-736.

Bijwaard, H., W. Spakman, and R. Engdahl, 1998. Closing the gap between regional and global travel time tomography, J. Geophys. Res., 103, pp.30,055–30,078.

Bohm M., G. Asch, Pak Fauzi, E.R. Flüh, K.S. Brotopuspito, H. Kopp, B.-G. Lühr, N.T. Puspito, A. Ratdomopurbo, W. Rabbel, D. Wagner, and *MERAMEX* Research Group, 2005. The *MERAMEX* Project - A Seismological Network in Central Java, Indonesia - Statusseminar des GEOTECHNOLOGIEN PRG. „Kontinentränder: Brennpunkte im Nutzungs- und Gefährdungspotenzial der Erde“, Session: SUNDAARC, GeoForschungsZentrum (GFZ) Potsdam, 09.-10. June, 2005

Bolfan-Casanova, Nathalie, 2007. Fuel for Plate Tectonics; Science, Vol. 315. no. 5810, pp. 338 - 339, [DOI: 10.1126/science.1137738].

Chadwick, J. P., 2008. Magma crust interaction in volcanic systems: Case studies from Merapi Volcano, Indonesia, Taupo Volcanic Zone, New Zealand, and Slieve Gullion, N. Ireland: PhD thesis, Trinity College Dublin, pp. 181.

Chadwick, J. P., V.R. Troll, C. Ginibre, D.Morgan, R. Gertisser, T.E. Waight, and J.P. Davidson, 2007. Carbonate Assimilation at Merapi Volcano, Java, Indonesia: Insight from Crystal Isotope Stratigraphy; Journal of Petrology, Vol 48, No. 9, pp. 1793-1812.

Costa, F., Andreastuti, S., Bouvet de Maisonneuve, C., Pallister, J,. 2013. Petrological insights into the storage conditions, and magmatic processes that yielded the centennial 2010 Merapi explosive eruption (this issue), http://dx.doi.org/10.1016/j.jvolgeores.2012.12.025.

Deegan, F.M., V.R. Troll, C. Freda, V. Misiti, J.P. Chadwick, 2011. Fast and furious: crustal CO2 release at Merapi volcano, Indonesia, Geology Today, 27 (2011), pp. 63–64

DeMets, C., R. Gordon, D. Argus, and S. Stein, 1990. Current plate motions, Geophys. J. Int., 101, pp.425-478.

Dzierma, Y., W. Rabbel, M. Thorwart, I. Koulakov, H. Wehrmann, K. Hoernle and D. Comte, 2012. Seismic velocity structure of the slab and continental plate in the region of the 1960 Valdivia (Chile) slip maximum—Insights into fluid release and plate coupling. Earth and Planetary Science Letters, 331, 164-176.

Engdahl, E.R., R. van der Hilst, and R. Buland, 1998. Global teleseismic earthquake relocation with improved travel times and procedures for depth determination, Bull. Seism. Soc. Am. 88, pp. 722–743.

Gertisser, R., and J. Keller, 2003. Temporal variations in magma composition at Merapi Volcano (Central Java, Indonesia): magmatic cycles during the past 2000 years of explosive activity. Journal of Volcanology and Geothermal Research, 123, pp. 1-23.

Gill, J.B., 1981, Orogenic Andesites and Plate Tectonics, Springer Verlag, Berlin.

Goes S., F. A. Capitanio & G. Morra, 2008. Evidence of lower-mantle slab penetration phases in plate motions, Nature 451, 981-984

Gorbatov, A., and B.L.N. Kennett, 2003. Joint bulk-sound and shear tomography for Western Pacific subduction zones, Earth and Planetary Science Letters 210, pp.527-543.

Gossler J., 2000. Teleseismic Observations at Merapi Volcano, Indonesia, DGG-Mitteilungen, Sonderband IV/2000, pp.17-22.

Hoffmann-Rothe, A., O. Ritter, and V. Haak, 2001. Magnetotelluric and geomagnetic modelling reveals zones of very high electrical conductivity in the upper crust of Central Java, Phys. Earth. Planet. Int., Vol. 1124/3-4, pp.131-151.

Husen, S., and E. Kissling, 2001. Postseismic fluid flow after the large subduction earthquake of Antofagasta, Chile, Geology, 29, pp. 847-850.

International Seismological Centre, 2001. Bulletin Disks 1-9 [CD-ROM], Internatl. Seis. Cent., Thatcham, United Kingdom.

Kennett, B.L.N., E.R. Engdahl, and R. Buland, 1995. Constraints on seismic velocities in the Earth from traveltimes, Geophys. J. Int., 122, pp.108-124.

Koulakov, I. (2011), High-frequency P and S velocity anomalies in the upper mantle beneath Asia from inversion of worldwide traveltime data, J. Geophys. Res., 116, B04301, doi:10.1029/2010JB007938.

Koulakov, I., Evgeniy I. Gordeev, Nikolay L. Dobretsov, Valery A. Vernikovsky, Sergey Senyukov, and Andrey Jakovlev, 2011a. Feeding volcanoes of the Kluchevskoy group from the results of local earthquake tomography - GEOPHYSICAL RESEARCH LETTERS, VOL. 38, L09305, doi: 10.1029/2011GL046957.

Koulakov, I.,N.L. Dobretsov, N.A. Bushenkova , A.V. Yakovlev, (2011b). Slab shape in subduction zones beneath the Kurile–Kamchatka and Aleutian arcs based on regional tomography results, Russian Geology and Geophysics 52, pp. 650–667

Koulakov, I., T. Yudistira, B.-G. Luehr, and Wandono, 2009a. P, S velocity and VP/VS ratio beneath the Toba caldera complex (Northern Sumatra) from local earthquake tomography. - Geophys. J. Int., doi: 10.1111/j.1365-246X.2009.04114.x.

Koulakov, I., A. Jakovlev, and B. G. Luehr, 2009b. Anisotropic structure beneath central Java from local earthquake tomography, Geochem. Geophys. Geosyst., (G3), 10, Q02011, doi:10.1029/2008GC002109.

Koulakov I., M.K. Kaban, M. Tesauro, and S. Cloetingh, 2009c, P and S velocity anomalies in the upper mantle beneath Europe from tomographic inversion of ISC data, Geophys. J. Int. 179, 1, p. 345-366. doi: 10.1111/j.1365-246X.2009.04279.x

Koulakov, I., M. Bohm, G. Asch, B.-G. Luehr, A. Manzanares, K. Brotopuspito, P. Fauzi, M.A. Purbawinata, N. Puspito, A. Ratdomopurbo, H. Kopp, W. Rabbel, E. Shevkunova, 2007. P and S velocity structure of the crust and the upper mantle beneath Central Java from local tomography inversion, J. Geophys. Res., 112, B08310, doi:10.1029/2006JB004712.

Koulakov, I., Sobolev, S.V., 2006. A tomographic image of Indian lithosphere break-off beneath the Pamir–Hindukush region, Geophys. J. Int. 164 (2), pp. 425–440.

Koulakov, I., S.V.Sobolev, and G. Asch, 2005. P- and S-velocity images of the lithosphere-asthenosphere system in the Central Andes from local-source tomographic inversion. Geophys. Journ. Int., 167, pp. 106-126.

Koulakov, I., Tychkov, S., Bushenkova, N., Vasilevsky, A., 2002. Structure and dynamics of the upper mantle beneath the Alpine–Himalayan orogenic belt, from teleseismic tomography. Tectonophys. 358 (1–4), pp. 77–96.

Levin V., Shapiro N., Park J., and Ritzwoller M. (2003) Seismic evidence for catastrophic slab loss beneath Kamchatka. Nature 418, pp. 763–767.

Maercklin, N., C. Riedel, W. Rabbel, U. Wegler, B.-G. Lühr, J. Zschau, 2000, Structural Investigation of Mt. Merapi by an Active Seismic Experiment, In: Deutsche Geophys. Gesellschaft-Mitteilungen, Sonderband

IV/2000, pp. 13-16.

Mei, Estuning Tyas Wulan, Franck Lavigne, Adrien Picquout, Edouard de Bélizal, Daniel Brunstein, Delphine Grancher, Junun Sartohadi, Noer Cholik, Céline Vidal, 2013. Lessons learned from the 2010 Evacuations at Merapi Volcano, Journal of Volcanology and Geothermal Research. (this issue)

Mierdel, K., H. Keppler, J. R. Smyth, and F. Langenhorst, 2007. Water Solubility in Aluminous Orthopyroxene and the Origin of Earth's Asthenosphere; Science, Vol. 315. no.5810, pp. 364 - 368, [DOI: 10.1126/science.1135422]

Müller, R. D., W. R. Roest, J.-Y. Royer, L. M. Gahagan, and J. G. Sclater, 1997. Digital isochrons of the world's ocean floor. *Journal of Geophysical Research, 102, 3211-3214, 1997*

Müller, A., and V. Haak, 2004. 3-D modeling of the deep electrical conductivity of Merapi volcano (Central Java): integrating magnetotellurics, intuction vectors and the effects of steep topography. Journal of Volcanology and Geothermal Research 138, pp.205-222.

Müller, M, A. Hördt & F.M. Neubauer, 2002. Internal structure of Mt. Merapi (Indonesia) derived from transient electromagnetic (LOTEM) data, JGR, 107, NO. B9, 2187, doi:10.1029/2001JB000148.

Nakajima, J., T. Matsuzawa, A. Hasegawa, and D. Zhao, 2001. Three-dimensional structure of Vp, Vs and Vp/Vs beneath northeastern Japan: Implication for arc magmatism and fluids, J.Geophys.Res., 106, pp.21843-21857.

Okada, T., and A. Hasegawa, 2000. Activity of deep low-frequency microearthquakes and their moment tensor in Northwestern Japan (in Japanese with English abstract), Bull. Volcanol. Soc. Jpn., 45, pp.47-63.

Okaya, D., S. Henrys, and T. Stern, 2002. "Super-gathers" across the South Island of New Zealand: double-sided onshore-offshore seismic imaging of a plate boundary, Tectonophysics, 355, pp.247-263.

Peacock, S. M., 2001. Are the lower planes of double seismic zones caused by serpentine dehydration in subducting oceanic mantle, Geology 29, pp.299-302.

Peacock, S.M., 1993. The importance of blueshist-eclogite dehydration reactions in subducting oceanic crust, Bull. Seis. Soc. Am., 105, pp.684-694.

Pesicek, J., Thurber C., Widiyantoro S., Engdhal E. R., DeShon H., 2008. Complex slab subduction beneath northern Sumatra, Geophys. Res. Lett., 35, L20303, doi: 10.1029/2008GL035262.

Poli, S., and M.W. Schmidt, 1995. H2O transport and release in subduction zones: Experimental constrains on basaltic and andesitic systems, J.Geophys. Res., 100, pp. 22299-22314.

Purbawinata, M.A., Ratdomopurbo, A., Sinulingga, I.K., Sumarti, S. & Suharno (Ed.), 1997. Merapi Volcano - A Guide Book, Volcanological Survey of Indonesia, Bandung, Indonesia, 64 pp..

Rahardjo, Wartono, Sukandarrumidi, Rosidi, H. M. D., 1995. Geologi lembar Yogyakarta skala 1:100.000. Pusat Penelitian dan Pengembangan Geologi, Bandung.

Ratdomopurbo, M. A. and G. Poupinet, 1995. Monitoring temporal change of seismic velocity in a volcano: application to the 1992 eruption of Mt. Merapi (Indonesia). Geophys. Res. Lett., 22, (7), pp. 775-778.

Reichert Chr., and B.-G. Luehr, 2005. High Risk Volcanism at the Active Margin of the SUNDAARC - BMBF GEOTECHNOLOGIEN Science Reports „Continental Margins - Earth's Focal Points of Usage and Hazard Potential", No. 5, pp.86-87.

Schurr B., G. Asch, A. Rietbrock, R. Trumbull, and C. Haberland, 2003. Complex patterns of fluid and melt transport in the central Andean subduction zone revealed by attenuation tomography, Earth and Planetary Science Letters, 215, 105-119.

Siebert, Lee, Simpkin, Tom, and Kimberly, Paul, 2010. Volcanoes of the World 3rd Edition, Smithsonian Institution, Washington D.C., 551 pp..

Simkin T., and L. Siebert, 1994. Volcanoes of the World, 2nd edition: Geoscience Press in association with the Smithsonian Institution Global Volcanism Program, Tucson AZ, pp.368.

Siswowidjoyo, S., Suryo, I., Yokoyama, I., 1995. Magma eruption rates of Merapi volcano, Central Java, Indonesia during one century (1890–1992). Bulletin of Volcanology 57, 111–116.

Smith, W.H.F., and D.T.Sandwell, 1997. Global seafloor topography from satellite altimetry and ship depth soundings, Science, 277, pp.1957–1962.

Supriyati Andreastuti, F. Costa, J. Pallister, Sri Sumarti, Sri Subandini, A. Heriwaseso, and Y. Kurniadi, 2011. Petrology and pre-eruptive conditions of the 2010 Merapi magma. EGU General Assembly 2011, Vol. 13, EGU2011-5150, Vienna

Surono, Phil. Jousset, J. Pallister, M. Boichu, M. F. Buongiorno, A. Budisantoso, F. Costa, S. Andreastuti, F. Prata, D. Schneider, L. Clarisse, H. Humaida, Sri Sumarti, Chr. Bignami, J. Griswold, S. Carn, C. Oppenheimer & F. Lavigne, 2012. The 2010 explosive eruption of Java’s Merapi volcano – a ‘100-year’ event Journal of Volcanology and Geothermal Research, v. 241-242, pp.121-135.

Syracuse, E. M., and G. A. Abers, 2006. Global compilation of variations in slab depth beneath arc volcanoes and implications - G3, Volume 7, Number 5, 23 May 2006

Tiede, C., A.G. Camacho, and C. Gerstenecker, 2005. J. Fernández: Modelling the density at Merapi volcano area, Indonesia, via the inverse gravimetric problem, Geochemistry, Geophysics, Geosystems (G3), 6(9), pp.1-13.

Toutain, J.-P., Sortino, F., Baubron, J.-C., Richon, P., Surono, Sumarti, S., Nonell, A.,, 2009. Structure and CO_2 budget of Merapi volcano during inter-eruptive periods. Bull. Volcanol. 71, 815-826, doi:10.1007/s00445-009-0266-x.

Untung, M., and Y. Sato, 1978. Gravity and geological studies in Java, Indonesia, Geological Survey of Indonesia and Geological Survey of Japan, A joint research program on regional tectonics of Southeast Asia Institute for transfer of industrial technology projects. Special publication, 6, 207 pp.

van Bemmelen, R.W. 1949. The Geology of Indonesia. Government Printing Office, Nijhoff, The Hague.

Wagner, D., I. Koulakov, W. Rabbel, B.-G. Luehr, A. Wittwer, H. Kopp, M. Bohm, G. Asch and the *MERAMEX* Scientists, 2007. Joint Inversion of Active and Passive Seismic Data in Central Java. Geoph. J. Int. 170, pp. 923–932.

Waltham, D., R. Hall, H. R. Smyth, C. J. Ebinger, 2008. Basin formation by volcanic-arc loading. GSA Special Paper: Formation and applications of the sedimentary record in arc collision zones (ed A Draut), GSA Special Papers, v. 436, pp. 11-26.

Wegler, U., B.-G. Lühr, R. Snieder, and A. Ratdomopurbo, 2006. Increase of shear wave velocity before the 1998 eruption of Merapi volcano (Indonesia), Geophys. Res. Lett., 33, L09303, doi:10.1029/2006GL025928.

Wegler, U., B.-G. Lühr, 2001. Scattering behaviour at Merapi volcano (Java) revealed from an active seismic experiment. –Geophys. J. Int., 145, pp. 579-592.

Wegler, U., B.-G. Lühr & A. Ratdomopurbo, 1999. A repeatable seismic source for tomography at volcanoes - Annali di Geofisica, 42, 3, pp. 565-571.

Westerhaus, M., B.-G. Lühr, M. Müller, G. Läufer, 2007. Inner structure and fluid transport at Merapi Volcano, Central Java – Festschrift zum 65. Geburtstag von Prof. Dr. Ing. Carl-Erhard Gerstenecker, Schriftenreihe der Fachrichtung Geodäsie Fachbereich Bauing.-wesen & Geodäsie, TU Darmstadt, ISBN 978-3-935631-17-4, Heft 28, pp 89-106, Dez. 2007

Widiyantoro, S., Kennett, B.L.N., Van der Hilst, R.D., 1999. Seismic tomography with P and S data reveals lateral variations in the rigidity of slabs, Earth and Planetary Science Letters, v. 173, pp. 91-100.

Zschau, J R. Sukhyar, M.A. Purbawinata, B.-G. Lühr, 2003. The Merapi-Project – Interdisciplinary Monitoring of a High-Risk Volcano as a Basis for an Early Warning System; in Early Warningsystems for Natural Disaster Reduction, Editors: J. Zschau, A. Küppers, Springer-Verlag, Berlin, Heidelberg, New York, pp.527-534.

Zschau, J. Sukhyar, R., M.A. Purbawinata, B.-G. Lühr; M. Westerhaus, 1998. Project MERAPI - Interdisciplinary Research at a High-Risk Volcano; DGG-Mitteilungen, Sonderband III/1998, pp.3-8.

Figures:

Figure 1. Map showing the investigation area of Central Java with all volcanoes, geological structures, and settlements mentioned in the text.

Figure 2. Distribution of the slab-related seismicity at Java. Event data are from the ISC catalogue for the period 1964-2002. Coloured zones highlight the occurrence of events in the four deepest depth intervals as indicated in the scale. Yellow triangles mark volcanoes with Lawu (LW), Sumbing (SMB), Sundoro (SUN), Dieng (DNG) volcanoes, and the red circle marks Merapi volcano (MRP).he black star marks the M=6.3 Bantul earthquake happened on 26 May 2006.

Figure 3. The upper panels show results of the tomographic inversion showing P and S-seismic models based on ISC catalogue data. The four lower panels show the results for P and S anomalies projected into the two vertical sections, one aligned to the west (W) and the other to the east of Merapi (E). The red circle marks Merapi volcano.

Figure 4. Local earthquakes recorded during the *MERAMEX* Project during 150 days (May to October 2004). (a) Map view. Sources are colour coded according to their depth. Triangles show the position of the *MERAMEX* seismic stations. The main volcanic complexes are outlined with black contours. (b) Horizontal cross section. Size and darkness of dots represent distance to the profile. Inferred upper limit of the slab and double seismic zone are highlighted with red lines.

Figure 5. Results of anisotropic inversion after five iterations in two horizontal depth slices. Colours indicate the isotropic velocity perturbations relative to AK 135 velocity model which are computed as average of four anisotropic parameters in each point. Vectors show directions of fast horizontal P velocities. Length of

vectors reflects difference between fastest and slowest horizontal velocities. The reference vector (10% of anisotropy) is shown below the left figure column. Volcanic complexes are marked for Lawu (LW), Sumbing (SMB), Sundoro (SUN), Dieng (DNG). The yellow star indicates the epicentre of the M=6.3 Bantul earthquake 2006. Profiles of two cross sections presented in Figure 6 are shown in maps. Black lines show the coast of Java and position of the main volcanic complexes, same as in Figure 2. Prominent is a strong negative velocity anomaly called MLA (Merapi-Lawu Anomaly).

Figure 6. Cross sections of anisotropic P and isotropic S models based on five iterations of the model. Positions of sections are shown in Figure 5. The anisotropy vectors for the P model are vertical if the vertical velocity variations are larger than the average horizontal perturbations and horizontal in the opposite case. The reference vector (6% of anisotropy) is shown in the left-bottom corner. Black dots show positions of the relocated sources within 30 km of the profile. Stronger anomalies close to model boundaries are of low significance.

Figure 7. Result of optimization for dρ/dV coefficients in the crust. Gravity map after Smith and Sandwell (1997) on the left and calculated gravity values derived from Vp and Vs velocities (on the right) showing a strong negative gravity anomaly in Central Java, extending to the east. The gravity anomaly fits well with the seismic velocity anomaly MLA (centered at approximately 7°S, 111°E).

Figure 8. Cross-section sketch of Merapi volcano according to Radomopurbo and Poupinet (1995) who postulated a shallow magma reservoir inside the edifice of Merapi based on an observed aseismic zone. Volcano tectonic events shown as circles are detected as a lower (VTA) and upper (VTB) cluster, respectively. The main chamber was inferred to be located beneath the VTA seismicity. The dots are intended to show the extent of magma.

Figure 9. Synoptic model showing the link between the subduction process and Merapi volcano. The background shows P velocities (color code is the same as in Figure 6). Yellow circles show distribution of local seismicity recorded within this study. Blue waved arrows indicate zone of fluid release from the slab. Brown dotted arrows mark the ascent paths of fluid and melt migration. Black dashed lines indicate V-shaped weakened zone with lower seismic velocity and higher seismicity which could be related to thrusting

caused by increasing friction on the upper surface of the slab. Shallow green area to the right of Merapi indicates the sediment cover above the MLA. We have little data to define the position of the Moho, thus it is shown with question marks.

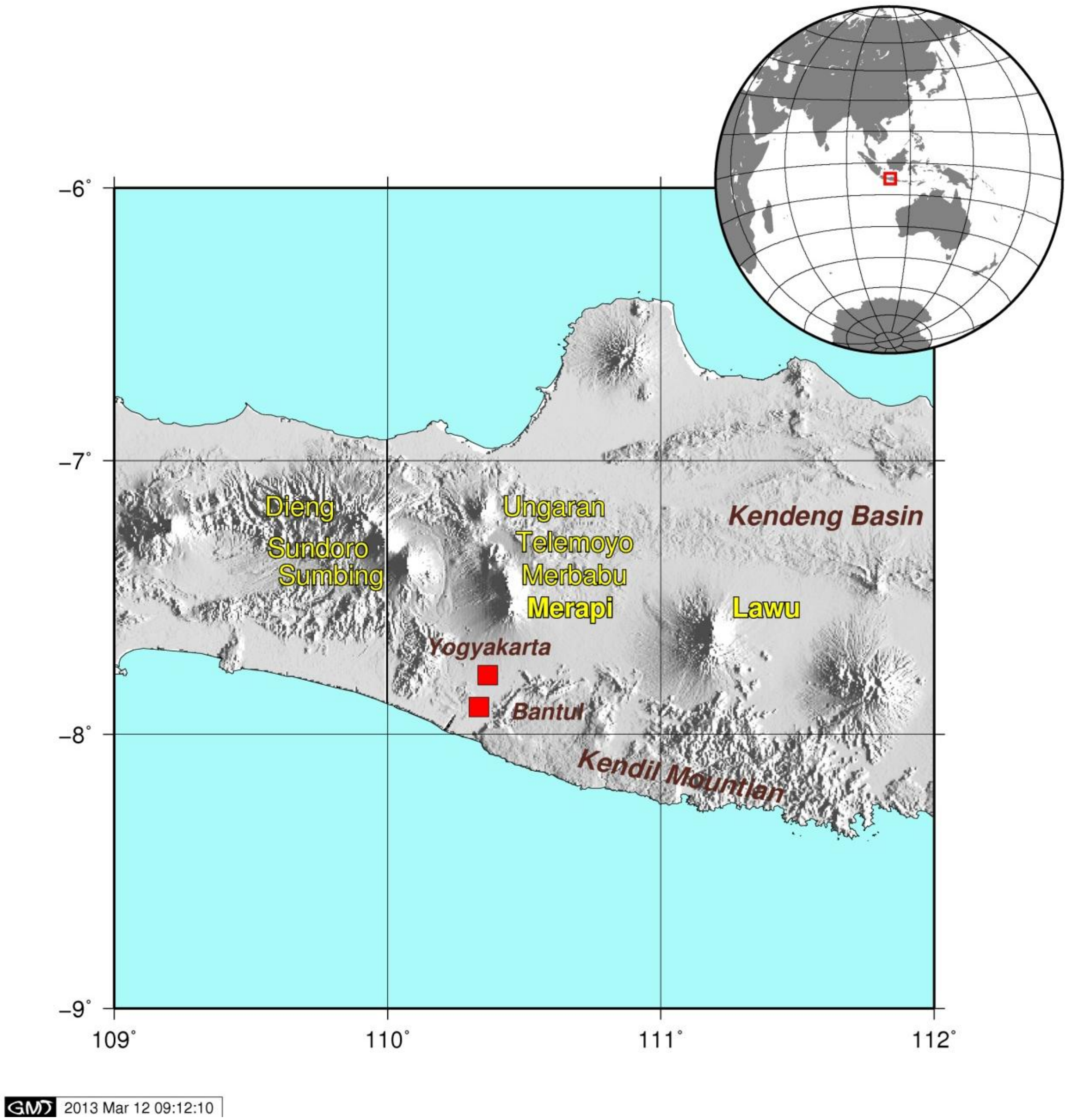
-6°
-7°
-8°
-9°
109°
110°
111°
112°
Dieng
Sundoro
Sumbing
Ungaran
Telemoyo
Merbabu
Merapi
Lawu
Kendeng Basin
Yogyakarta
Bantul
Kendil Mountian
GMT 2013 Mar 12 09:12:10

Fig. 1

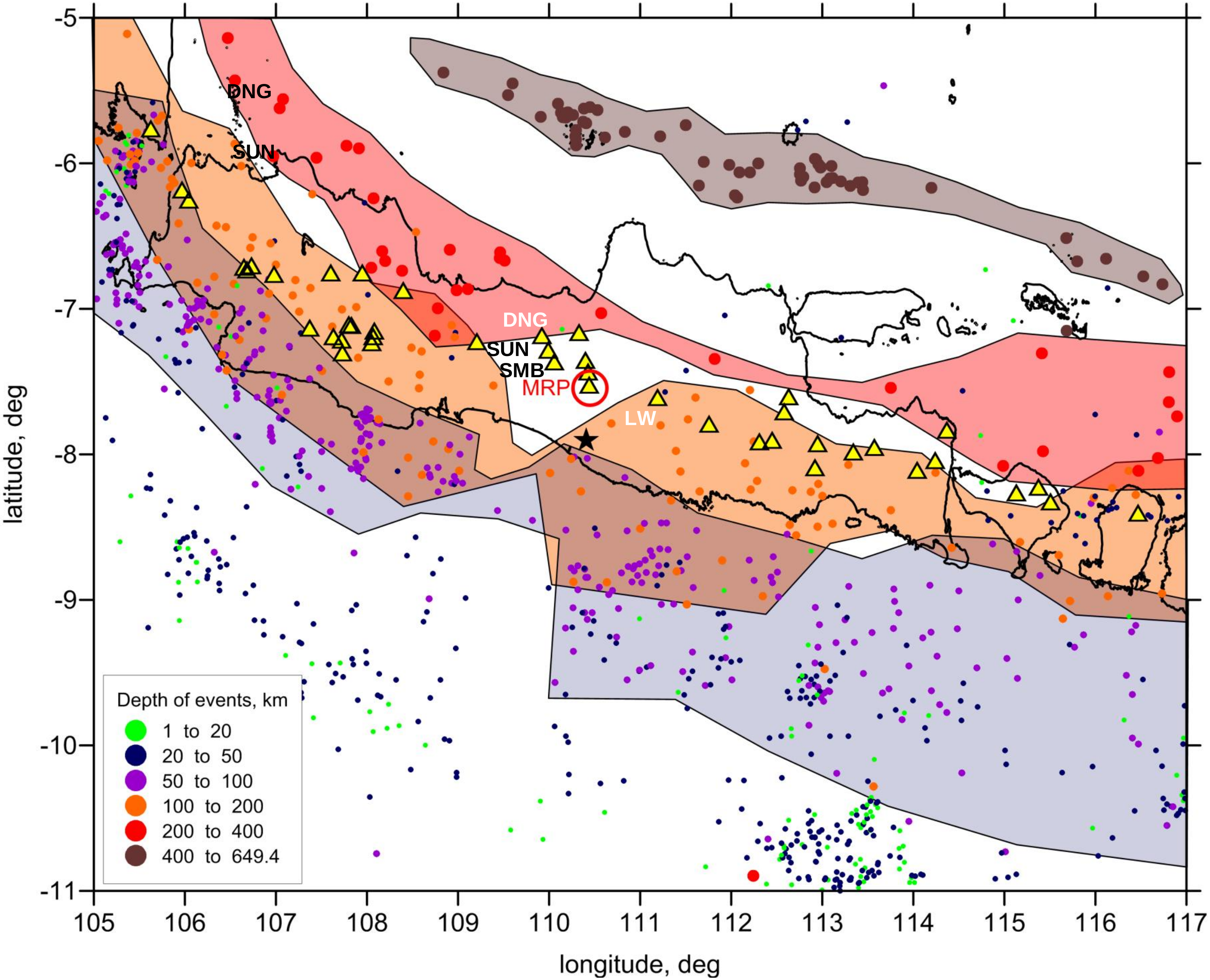

-5
-6
-7
-8
-9
-10
-11
latitude, deg
105
106
107
108
109
110
111
112
113
114
115
116
117
longitude, deg
DNG
SUN
DNG
SUN
SMB
MRP
LW
Depth of events, km
1 to 20
20 to 50
50 to 100
100 to 200
200 to 400
400 to 649.4

Fig. 2

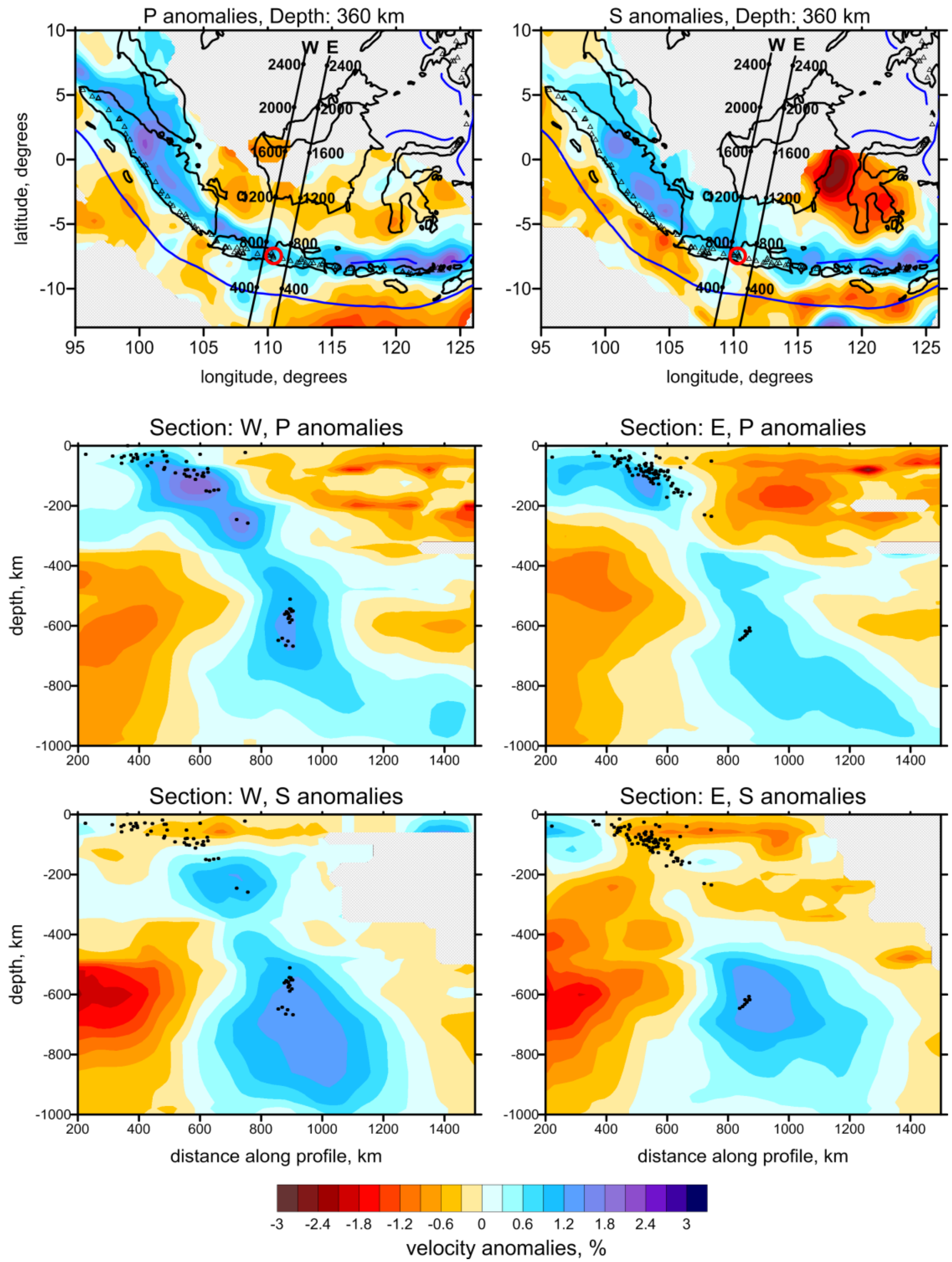

P anomalies, Depth: 360 km
S anomalies, Depth: 360 km
latitude, degrees
longitude, degrees
W E
2400
2000
1600
1200
800
400
Section: W, P anomalies
Section: E, P anomalies
Section: W, S anomalies
Section: E, S anomalies
depth, km
distance along profile, km
velocity anomalies, %

Fig. 3

Fig. 4

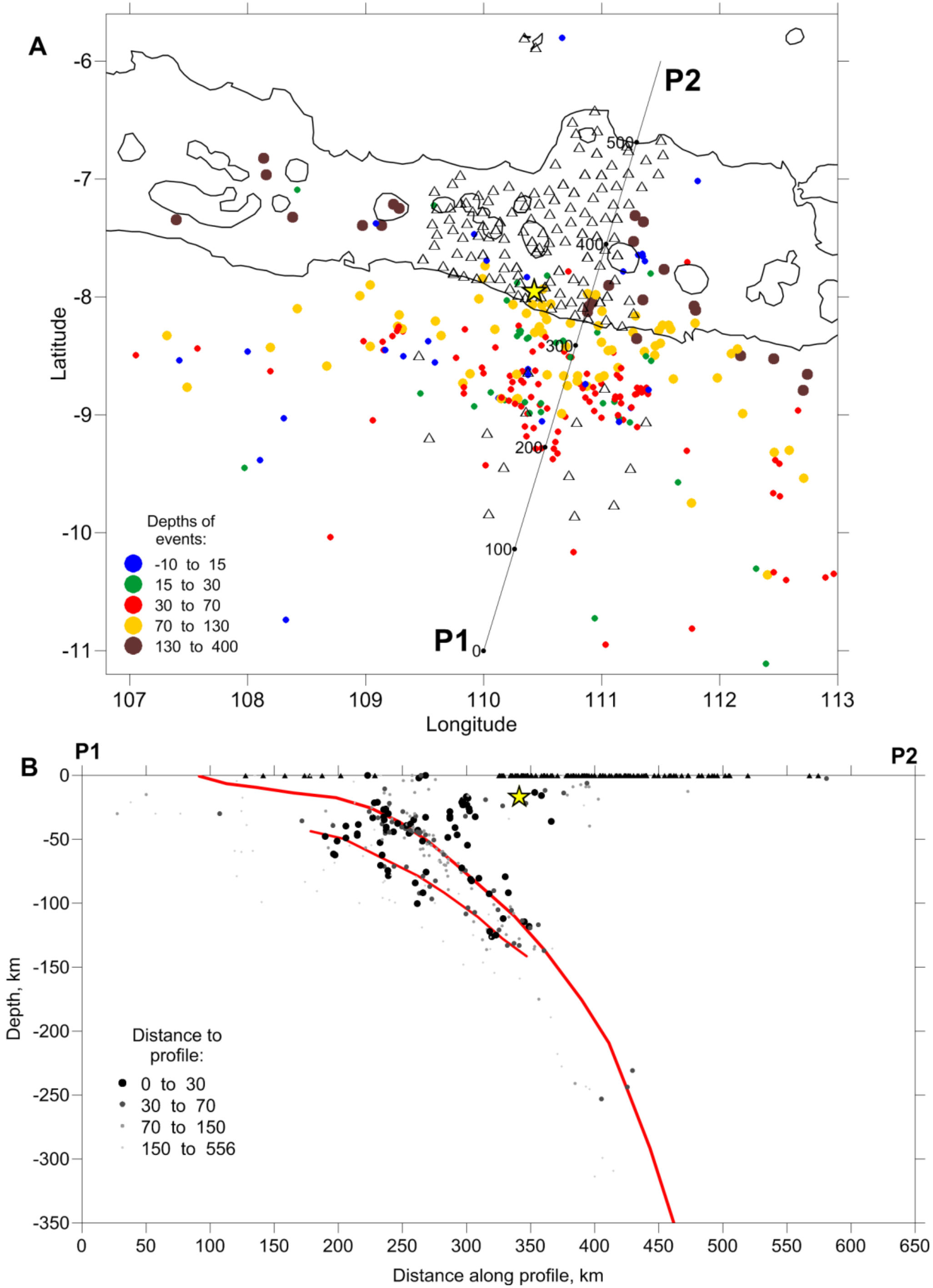

A
P2
P1
500
400
300
200
100
0
-6
-7
-8
-9
-10
-11
Latitude
107
108
109
110
111
112
113
Longitude
Depths of events:
-10 to 15
15 to 30
30 to 70
70 to 130
130 to 400
B
P1
P2
Depth, km
0
-50
-100
-150
-200
-250
-300
-350
0
50
100
150
200
250
300
350
400
450
500
550
600
650
Distance along profile, km
Distance to profile:
0 to 30
30 to 70
70 to 150
150 to 556

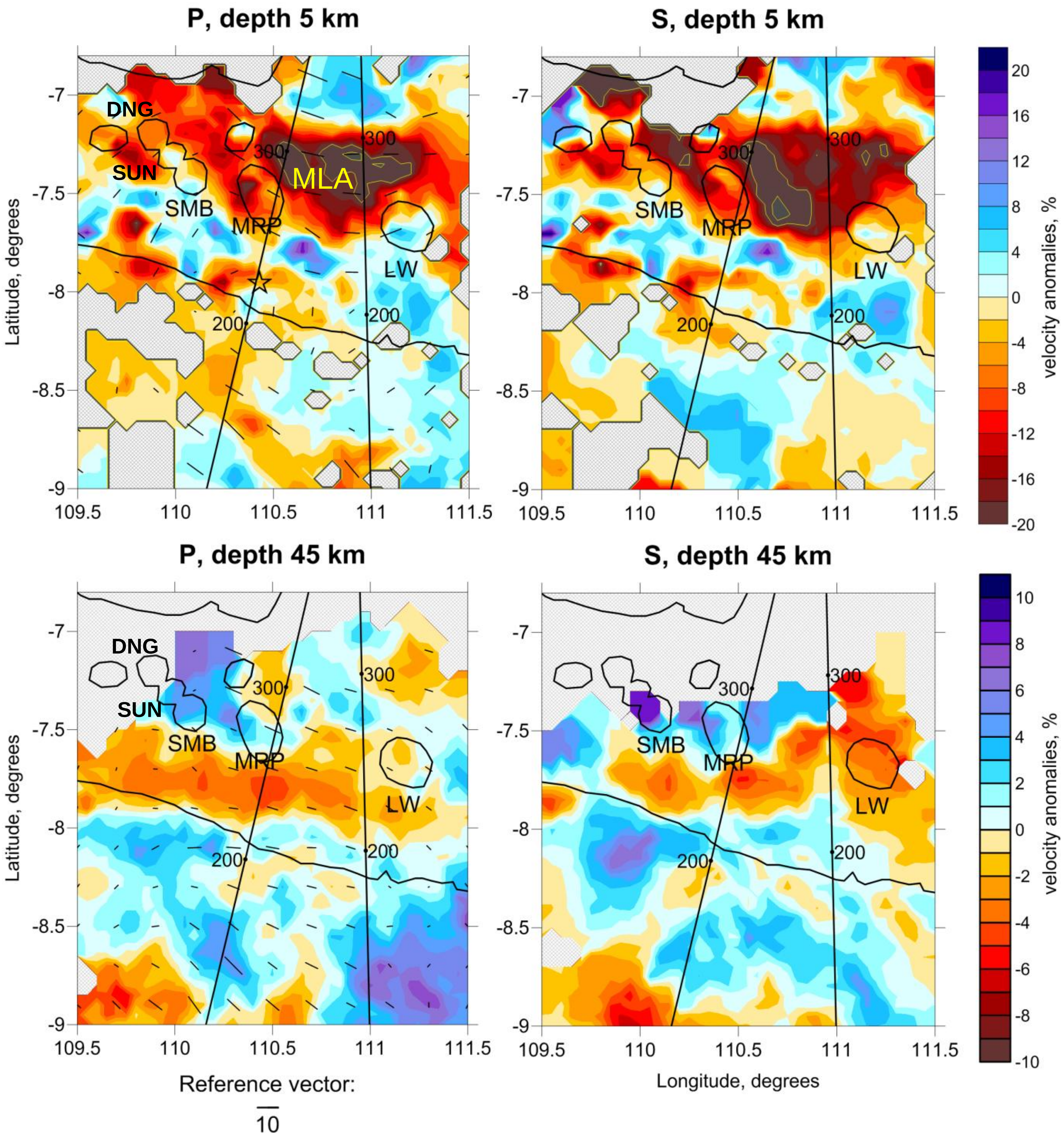

P, depth 5 km
S, depth 5 km
P, depth 45 km
S, depth 45 km
DNG
SUN
SMB
MRP
MLA
LW
300
200
Latitude, degrees
Longitude, degrees
velocity anomalies, %
Reference vector:
10

Fig. 5

Fig. 6

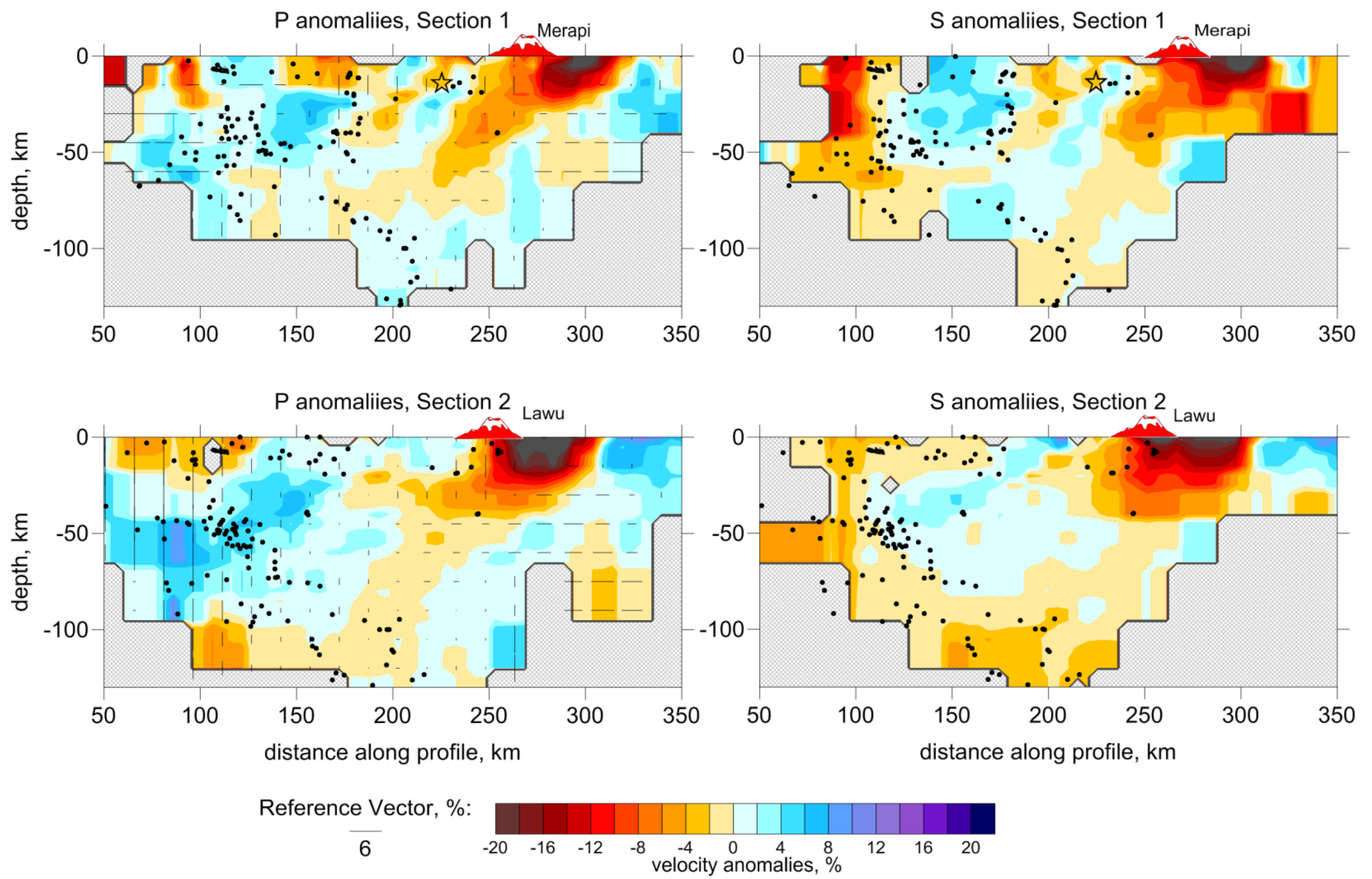

P anomaliies, Section 1
Merapi
S anomaliies, Section 1
Merapi
P anomaliies, Section 2
Lawu
S anomaliies, Section 2
Lawu
depth, km
distance along profile, km
Reference Vector, %:
6
velocity anomalies, %

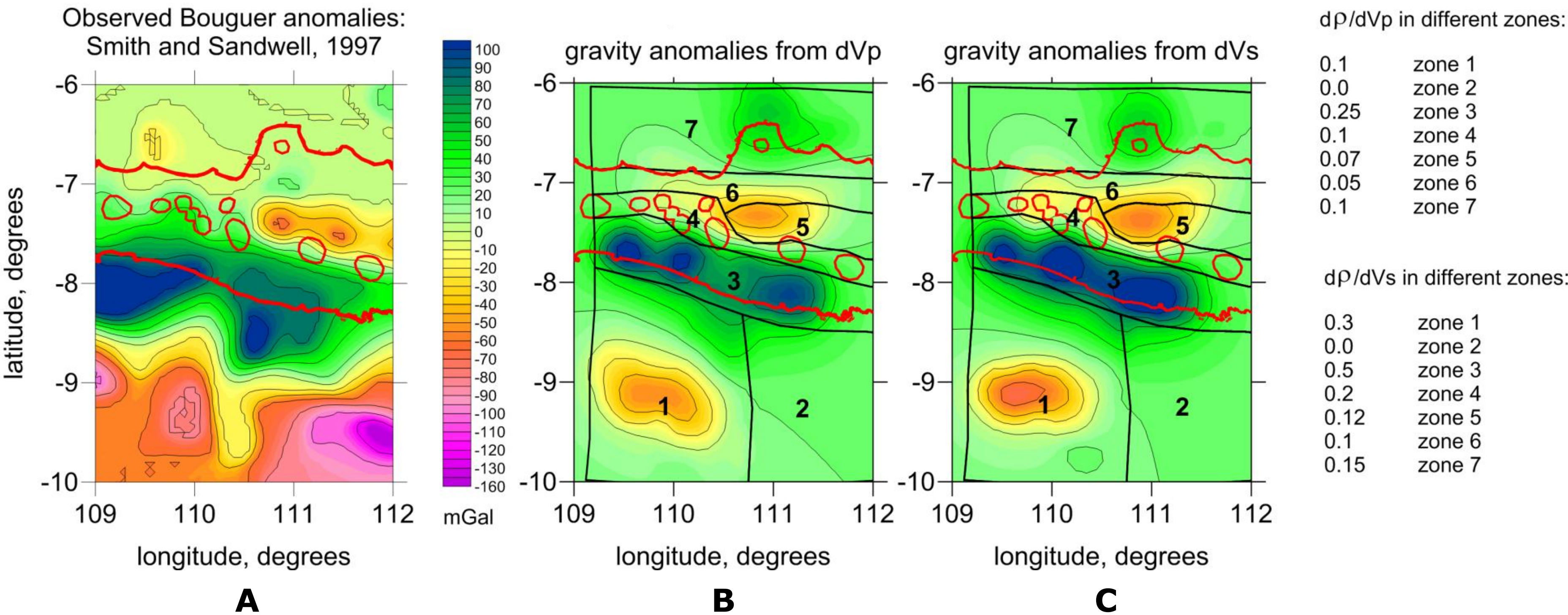
Observed Bouguer anomalies:
Smith and Sandwell, 1997
latitude, degrees
longitude, degrees
mGal
100
90
80
70
60
50
40
30
20
10
0
-10
-20
-30
-40
-50
-60
-70
-80
-90
-100
-110
-120
-130
-160
A
gravity anomalies from dVp
B
gravity anomalies from dVs
C
dρ/dVp in different zones:
0.1 zone 1
0.0 zone 2
0.25 zone 3
0.1 zone 4
0.07 zone 5
0.05 zone 6
0.1 zone 7
dρ/dVs in different zones:
0.3 zone 1
0.0 zone 2
0.5 zone 3
0.2 zone 4
0.12 zone 5
0.1 zone 6
0.15 zone 7

Fig. 7

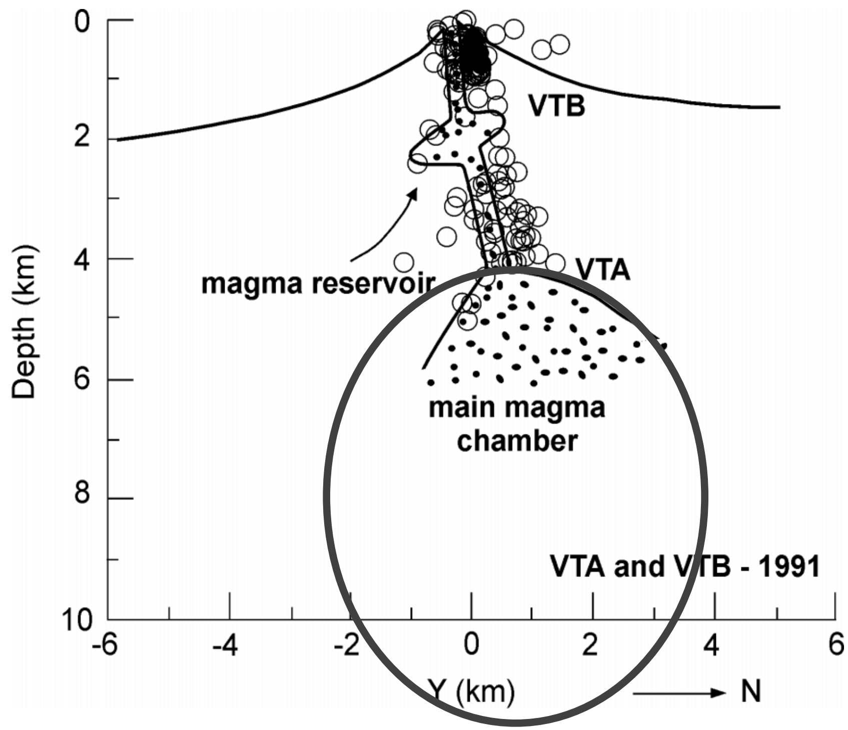

VTB
VTA
magma reservoir
main magma
chamber
VTA and VTB - 1991
Depth (km)
Y (km)
N

Fig. 8

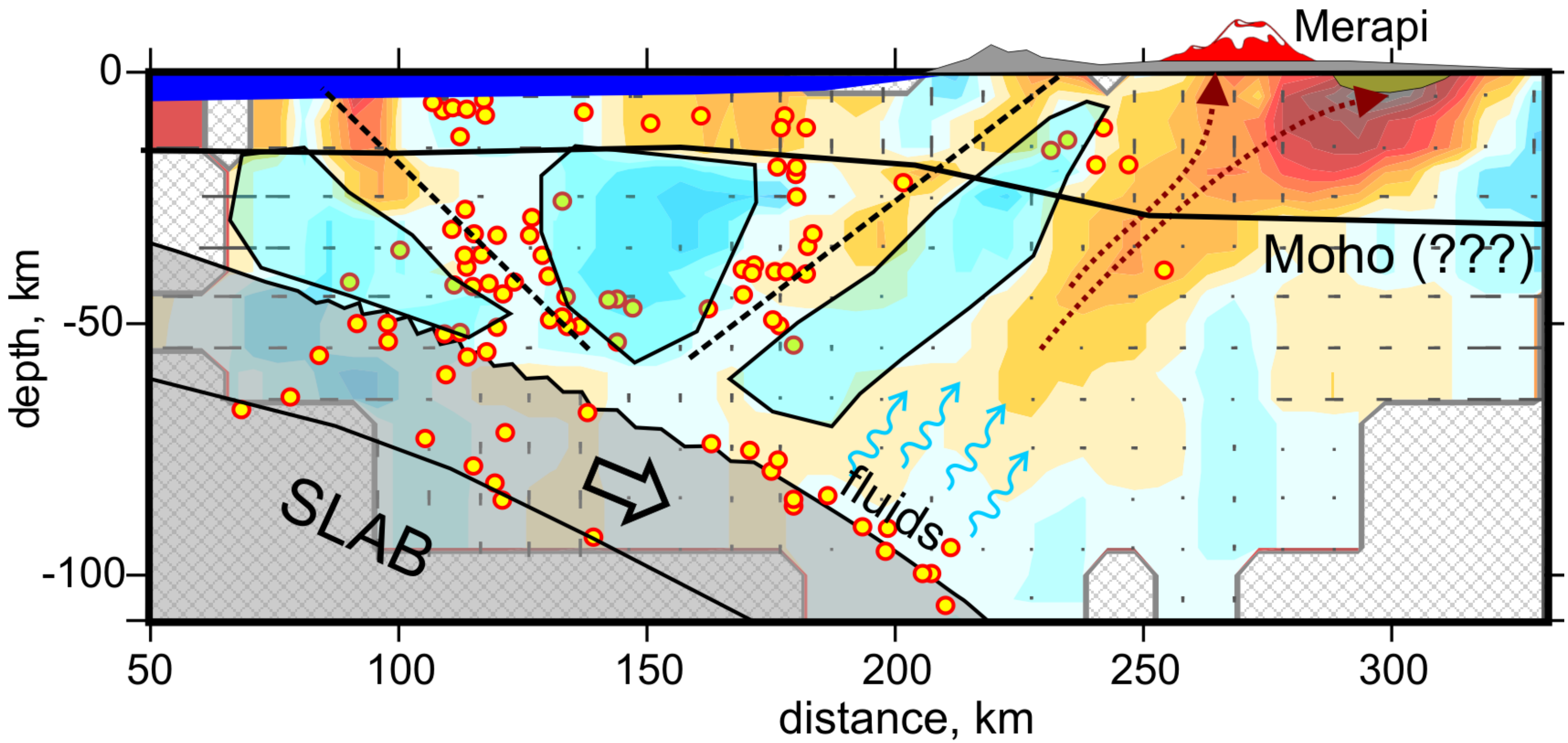

Merapi
0
-50
-100
depth, km
Moho (???)
fluids
SLAB
50
100
150
200
250
300
distance, km

Fig. 9